molecular pharmaceutics

Article

pubs.acs.org/molecularpharmaceutics

Pharmacokinetics of an Injectable Modified-Release 2-Hydroxyflutamide Formulation in the Human Prostate Gland Using a Semiphysiologically Based Biopharmaceutical Model

Erik Sjögren,[†] Teuvo L. Tammela,[‡] Bo Lennernäs,[§] Kimmo Taari,[∥] Taina Isotalo,[⊥] Lars-Åke Malmsten,[¶] Niklas Axén,[¶] and Hans Lennernäs*[,†,¶]

[†]Department of Pharmacy, Uppsala University, SE-751 23 Uppsala, Sweden

[‡]Department of Urology, Tampere University Hospital, 33520 Tampere, Finland

[§]Department of Oncology, Göteborg University, 411 37 Gothenburg, Sweden

[∥]Department of Urology, Helsinki University Hospital and University of Helsinki, 00100 Helsinki, Finland

[⊥]Department of Urology, Lahti Central Hospital, FIN-15101 Lahti, Finland

[¶]LIDDS AB, SE-252 20 Helsingborg, Sweden

ABSTRACT: The local distribution of 2-hydroxyflutamide (2-HOF) in prostate tissue after a single intraprostatic injection of a novel parenteral modified-release (MR) formulation in patients with localized prostate cancer was estimated using a semiphysiologically based biopharmaceutical model. Plasma concentration−time profiles for 2-HOF were acquired from a phase II study in 24 patients and the dissolution of the MR formulation was investigated in vitro. Human physiological values and the specific physicochemical properties of 2-HOF were obtained from the literature or calculated via established algorithms. A compartmental modeling approach was adopted for tissue and blood in the prostate gland, where the compartments were modeled as a series of concentric spherical shells contouring the centrally positioned depot formulation. Discrete fluid connections between the blood compartments were described by the representative flow of blood, whereas the mass transport of drug from tissue to tissue and tissue to blood was described by a one-dimensional diffusion approximation. An empirical dissolution approach was adopted for the release of 2-HOF from the formulation. The model adequately described the plasma concentration−time profiles of 2-HOF. Predictive simulations indicated that the local tissue concentration of 2-HOF within a distance of 5 mm from the depot formulation was approximately 40 times higher than that of unbound 2-HOF in plasma. The simulations also indicated that spreading the formulation throughout the prostate gland would expose more of the gland and increase the overall release rate of 2-HOF from the given dose. The increased release rate would initially increase the tissue and plasma concentrations but would also reduce the terminal half-life of 2-HOF in plasma. Finally, an in vitro−in vivo correlation of the release of 2-HOF from the parenteral MR formulation was established. This study shows that intraprostatic 2-HOF concentrations are significantly higher than systemic plasma concentrations and that increased distribution of 2-HOF throughout the gland, using strategic imaging-guided administration, is possible. This novel parenteral MR formulation, thus, facilitates good pharmacological effect while minimizing the risk of side effects.

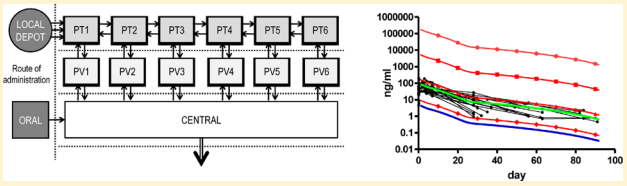

KEYWORDS: *prostate cancer, 2-hydroxyflutamide, Liproca Depot, physiological modeling, drug delivery*

■ INTRODUCTION

Globally, almost one million men are diagnosed with prostate cancer (PC) each year, with about 275 000 dying as a consequence.[1] Endogenous androgens, such as testosterone and its more potent metabolite dihydrotestosterone, are required for PC to advance and proliferate. PC is the second most frequently diagnosed cancer in developed countries, and the third most common cause of death from cancer in men. Clinically, PC is 80−90% diagnosed as a local disease. In a recent population-based cohort study of 45 440 Californian men with clinically localized PC, the most common primary treatment was surgery (40%), followed by radiotherapy (29%), conservative management (21%), and androgen deprivation therapy (ADT) (9.8%).[2] Patients who undergo prostatectomy or radiotherapy risk associated morbidity, and nearly 75% of all American men treated with either or both of these methods experience a biochemical recurrence, that is, increasing concentrations of prostate specific antigen (PSA).[3] In the Californian study, neoadjuvant ADT was administered significantly more often to men who received primary radiotherapy (40.8%) than to those treated with surgery (13.1%).[2] Neoadjuvant ADT is known to improve survival in patients receiving radiation therapy for PC.[4,5] However, systemic use of

Received: April 16, 2014
Revised: July 1, 2014
Accepted: July 23, 2014

primary ADT or oral antiandrogen treatment in patients with low-risk PC has not increased survival because of increased mortality from cardiovascular events.[6−9] Extensive side effects, such as metabolic syndrome, increased incidence of cardiovascular events, osteoporosis, sexual dysfunction, and gynecomastia, have been reported.[10] An effective local hormonal treatment with an improved side effect profile would be a welcome alternative to active surveillance and systemic ADT for patients with low-risk PC.

The injection of a modified-release (MR) formulation directly into the prostate gland is an attractive treatment approach that could improve efficacy and safety outcomes compared to systemic ADT treatments.[11] A novel parenteral MR formulation containing the antiandrogen 2-hydroxyflutamide (2-HOF) has been investigated in several preclinical and clinical studies.[12] The formulation contains a calcium sulfate drug carrier that has been modified at a microstructural level to make it bioresorbable and 2-HOF as the active pharmaceutical ingredient (API). 2-HOF is the pharmacologically active main metabolite of the androgen receptor antagonist flutamide.[13] After intraprostatic administration of this parenteral MR formulation into one lobe of the gland, systemic and local spatiotemporal exposure to 2-HOF will be determined by the rate of in vivo release from the depot along with (patho)physiological aspects such as membrane transport, tissue binding, blood flow, and metabolism. In both healthy and tumor-affected prostate tissue, drug disposition is determined by the rate and extent of transport through the vascular space and across the microvessel walls and diffusion through the tissue interstitium.[14] Physiologically based pharmacokinetic and biopharmaceutical modeling is a suitable method for investigating drug disposition in complex and multiparameter in vivo systems.[15]

The primary objective of this investigation was to estimate the local distribution of 2-HOF from this novel MR intraprostatic formulation by developing a semiphysiologically based biopharmaceutical (PBBP) model. This model is designed to provide concentration−time profiles for 2-HOF in plasma and prostate tissue (PT). In addition, the intention was to use this model to perform predictive simulations of the effects of dose escalation, degeneration of blood vessels (antiangiogenesis) and dissemination of the formulation through the prostate gland (i.e., developing an administration strategy). Finally, we wished to establish the in vitro−in vivo correlation (IVIVC) for the release of 2-HOF from the investigated MR formulation.

■ MATERIALS AND METHODS

Description of the Study Product: Liproca Depot. Liproca Depot is a parenteral MR product comprising two sterile components: an aqueous solution of 0.25% sodium carboxy methylcellulose (Liproca Diluent CMC, 4.0 mL) in a glass vial and a dry powder (Liproca Powder, 4.0 g), consisting of microstructurally modified calcium sulfate and the API 2-HOF in a specially designed syringe equipped with a mixing unit. Prior to administration, the diluents and the powder are mixed to a paste under aseptic conditions, and the paste is administered into the prostate gland under ultrasonic guidance. After injection of the paste, the formulation solidifies in vivo to form multiple small depot units in the prostate gland tissue from which 2-HOF is released as the carrier material slowly dissolves and disappears. These small, cured depot units have a two-phase microstructure comprising dense, compressed, nonporous (slow release) grains in a porous, noncompressed (faster release) matrix (Figure 1). Both MR phases contain 2-HOF. The porous grains contain 57% of the total 2-HOF content and the nonporous grains contain 43%. The porous and nonporous fractions are designed to release 2-HOF during approximately 2−3 and 16−20 weeks, respectively. Importantly, the calcium sulfate in this formulation is radiopaque, which facilitates the accurate transrectal ultrasound (TRUS)-guided administration of the formulation into the prostate gland.

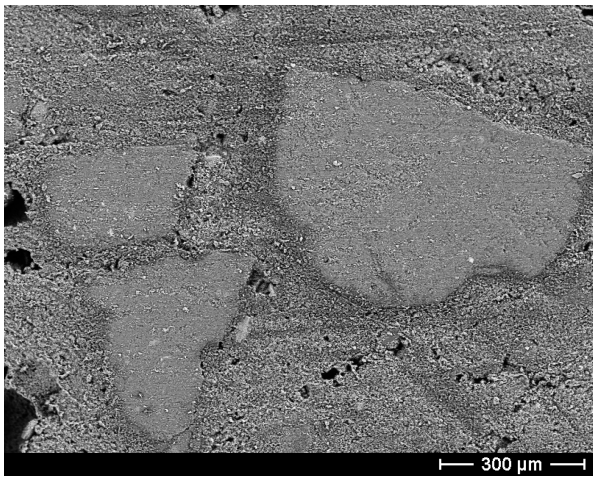

Figure 1. Electron microscopy image of the microstructure by a cross section of the solidified formulation showing dense nonporous granules in the porous matrix.

In Vitro Release of 2-HOF from the Depot Formulation. The solid and liquid components, Liproca Diluent CMC and Liproca Powder, were mixed to formulate the injectable paste. Four depot units, each weighing 0.3 g, were cured in air and each unit was placed in a beaker containing 300 mL of 0.9% NaCl. The in vitro dissolution test was performed over 21 weeks (147 days); samples of size 20 mL were withdrawn from the dissolution medium at designated time points. An equivalent volume of fresh dissolution medium was added to the beaker after each sampling and subsequent 2-HOF concentration measurements were adjusted accordingly. The dissolution medium was not stirred continuously, as this would not reflect the physiological and hydrodynamic environment of either the benign/malign tumor tissue or healthy PT. However, before each sampling, the in vitro medium was carefully and adequately stirred by gentle agitation to ensure equilibrium.

Clinical Study Design and Preparation of the Formulation in the Clinic. Plasma 2-HOF concentration−time profiles were obtained from an open, multicenter, clinical phase II study in 24 patients with localized PC (T1-T2).[16] The patients were monitored for 12 weeks (84 days) after a single individualized dose of Liproca Depot into one lobe of the prostate gland. The mean volume of the formulation injected was 3.6 mL (range 2.0−7.8 mL), corresponding to a mean 2-HOF dose of 720 mg (range 400−1560 mg). Liproca Depot was prepared under aseptic conditions via two consecutive mixing steps. First, 3.3 mL of the Liproca Diluent CMC was withdrawn from the vial and transferred to the Liproca Powder syringe (already loaded with 4.0 g of powder). The two components were thoroughly mixed in the powder syringe to form a paste. The prepared paste was then transferred to the original diluent syringe mounted onto the specially designed

injection applicator. When the applicator needle was positioned in the selected part of the prostate gland using standard TRUS guidance equipment, the paste was injected while simultaneously slowly withdrawing the needle from the distal starting point in the gland. The administration and distribution of the dose was continuously monitored with the ultrasound equipment. The mean prostate volume in the patient group, measured with the same TRUS equipment, was 48.1 mL. This value was used in the semi-PBBP model.

Plasma samples for the pharmacokinetic (PK) assessment of 2-HOF were taken on the day of injection (preinjection and 2, 4, and 6 h post injection) and after 1, 4, 8, and 12 weeks. The blood samples were centrifuged (at 1000*g*) for 15 min and immediately frozen as plasma at −20 °C. The plasma samples were transferred deep-frozen to Statens Veterinärmedicinska Anstalt (SVA, Uppsala, Sweden) for analysis.

Analytical Methods for Determining 2-HOF Concentrations. The method for quantitative determination of 2-HOF concentrations in human plasma using liquid chromatography coupled to tandem mass spectrometry (LC−MS/MS) was developed and validated at SVA (Uppsala, Sweden). The analysis was carried out by LC−MS/MS with negative electrospray ionization [LC Mass spectometer: TSQ Quantum Ultra (inv. no: 241); TSQ Quantum 1.4; Surveyor MS, Pump 1.01.3300]. The data acquisition mode was set to Selected Reaction Monitoring. The results were calibrated using the chromatographic peak area ratio (analyte/internal standard 2*H*6-hydroxy-flutamide) as a function of the 2-HOF plasma concentration. Tuning was performed on sensitivity optimization for the SRM transition m/z 291 ⇒ 205 for 2-HOF $[\text{M-H}]^-$.

The plasma samples were prepared by alkaline liquid−liquid extraction, followed by isolation and evaporation of the organic phase and reconstitution of the sample. A total of 500 μL of plasma, 200 μL of water, and 500 μL of 1.0 M sodium carbonate were mixed with each sample and 4.0 mL of hexane/dichloromethane (4:1) was added. The mixture was shaken in a vortex mixer for 3 min (1650 pulse) and then centrifuged at 3500*g* for 10 min. The organic phase was collected and evaporated to dryness under a gentle stream of nitrogen at 55 °C. The dry sample was reconstituted in 100 μL of 0.1% formic acid (aq), vortexed for 10 s, and the reconstituted sample was then transferred to a vial and injected onto the LC−MS/MS system. The validated concentration interval for quantification of 2-HOF in plasma was 0.5−500 ng/mL.

Theoretical Explanation of the Release of 2-HOF from the Depot Formulation. The release of a drug from a pharmaceutical formulation is traditionally regarded to be limited by either the diffusion rate or the dissolution rate and several theoretical analytical solutions to a wide range of formulations have been proposed.[17,18] An empirical approach was deployed in this study in order to develop a model that explained the complete release of 2-HOF from the investigated MR formulation where the drug release was determined by the composition and characteristics of the formulation. This approach was based on the Noyes−Whitney Equation (eq 1)[19]

$$\frac{dW}{dt} = \frac{DA\Delta C}{L} \tag{1}$$

where the rate of movement of the drug (weight W) from the solid depot to solution (dW/dt) was determined by the surface area of the formulation (A), the diffusion constant of the drug (D), the difference in concentration between the surface and the bulk of the depot (ΔC) and the thickness of the diffusion layer (L).

Assuming that the MR formulation forms one or several perfect sphere(s) that shrink symmetrically throughout the dissolution process and that the volume of the MR formulation is related to the amount of 2-HOF in the formulation, A is proportional to $W^{2/3}$. Assuming further that the release of 2-HOF from the drug depot is determined by the dissolution of the formulation and not by D, ΔC or L, these parameters can be substituted by a release rate constant (k). Under these assumptions, the Noyes−Whitney equation was reformulated as eq 2

$$\frac{dW}{dt} = kW^{2/3} \tag{2}$$

Similar reformulations of the Noyes−Whitney equation have been reported previously for different applications.[20−22]

Modeling. *In Vitro Release of 2-HOF from the Depot Formulation.* It appears reasonable to assume that 2-HOF is primarily released from this formulation via two different mechanisms: one represented by the fraction of 2-HOF that is incorporated and bound into the formulation matrix, the release of which is therefore dependent on wetting and dissolution/pore formation in the matrix, and the other represented by the fraction of 2-HOF that is released from the nonporous part of the formulation. The total release rate was thus described as the sum of two discrete and simultaneous release mechanisms (eq 3).

$$\frac{dW_{tot}}{dt} = \frac{dW_p}{dt} + \frac{dW_{np}}{dt} = k_p W_p^{2/3} + k_{np} W_{np}^{2/3} \tag{3}$$

where the subscripts tot, p and np refer to total, porous and nonporous (dense), respectively.

The porous and nonporous formulation components were allocated 57% and 43% of the total amount of 2-HOF, respectively, to represent the composition of the formulation.

A common feature of parenteral depot formulations is an initial unintended burst of readily available API on the outer surfaces of the formulation, which are in direct contact with the surrounding tissue fluids.[23,24] This initial release was kept as low as possible in this MR formulation, but the extent of the fraction released was nonetheless investigated by modeling the porous part as incorporating two separate release processes, giving a total of three simultaneous release mechanisms, as described by eq 4

$$\frac{dW_{tot}}{dt} = \frac{dW_{p-ub}}{dt} + \frac{dW_{p-b}}{dt} + \frac{dW_{np}}{dt} = k_{p-ub} W_{p-ub}^{2/3} + k_{p-b} W_{p-b}^{2/3} + k_{np} W_{np}^{2/3} \tag{4}$$

where the subscripts p−ub and p−b refer to unbound drug in the porous compartment (readily available at the surfaces, i.e., the burst dose) and bound drug in the porous compartment (enclosed in the matrix), respectively.

In Vivo Release of 2-HOF from the Depot Formulation. The in vivo analysis was carried out using the most promising release model from analysis of the in vitro data. However, as the in vivo solidification process occurs under moist conditions within the prostate gland, in contrast to the in vitro experiments where the formulation was cured in normal air, it was hypothesized that the in vivo release pattern might be somewhat different from the in vitro pattern. The presence of tissue and

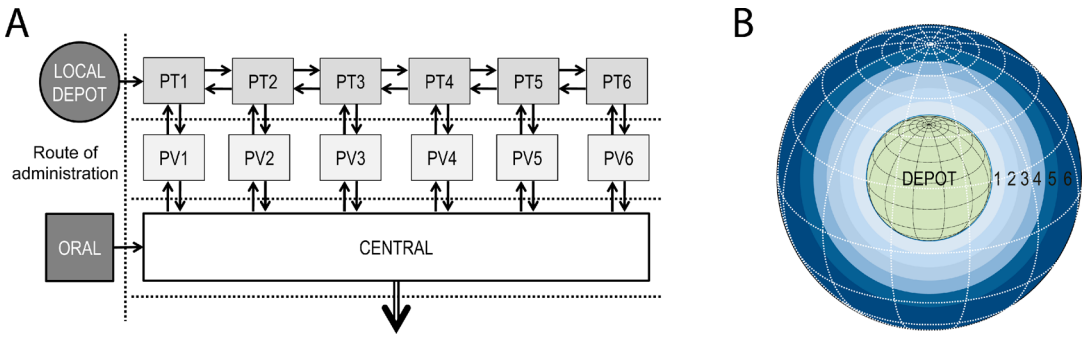

Figure 2. (A) Schematic representation of the semiphysiologically based biopharmaceutical (PBBP) model developed to describe the prostatic tissue disposition and plasma concentrations of 2-HOF. The compartmental depiction includes prostate tissue (PT), the prostate vascular compartments (PV), the central PK compartment (i.e., systemic blood), and the connections between compartments indicated by arrows. (B) Schematic depiction of the prostate tissue shell approximation model used in the semi-PBBP model. The PT compartments are numbered 1 to 6. Data such as volumes and distances within the prostate, input into the semi-PBBP model, were estimated based on this model approach.

Table 1. Physiological Data for the Prostate Used in the Semi-Physiologically Based Biopharmaceutical Model[a]

prostate compartment	ShTh (cm)	PLd (cm)	PLs (cm)	PV (ml)	PAr (cm^2)	PBV (ml)	PBQ (ml min^{-1})	PBAr (cm^2)
P1	0.20	0.10	0.20	2.8	17	0.053	3.9	190
P2	0.20	0.30	0.20	3.9	23	0.075	5.5	260
P3	0.20	0.50	0.20	5.3	30	0.10	7.3	350
P4	0.20	0.70	0.20	6.8	39	0.13	9.5	460
P5	0.20	0.90	0.28	8.6	48	0.16	12	580
P6	0.36	1.2		21	67	0.39	29	1400
Total	1.4			48			67	

[a]ShTh = the thickness of the prostate tissue compartment shell, PV = the volume of the prostate tissue compartment, PAr = the area of the prostate tissue compartment, PLs = the mean distance between the prostate tissue compartment shells, PLd = the mean distance from the prostate tissue compartment to the depot, PBV = the volume of the prostate blood compartment, PBQ = the rate of blood flow in the prostate blood compartment, and PBAr = the area of the prostate blood compartment.

tissue fluids could affect both the porosity and the surface of the formulation. As a consequence, the in vivo release model was described by in vivo-specific parameters, whereas the release model structure was in accordance with the conclusions from the in vitro analysis.

Physiological Modeling of Intraprostatic Drug Delivery. *Semi-PBBP Model Structure A.* The prostatic gland in the semi-PBBP model was constructed of six tissue and six blood compartments with discrete connections between compartments, as displayed in Figure 2A. Each compartment was allocated an appropriate physiological volume to convert the amount of 2-HOF in the compartment to a corresponding concentration. The rate of the mass transport of 2-HOF from and to the PT compartments was described in terms of clearances (CL, unit: volume × $time^{-1}$) based on a drug-specific multicellular layer diffusion coefficient.[25,26] The connections between vascular compartments were described by the representative blood flows, where each prostate vascular compartment was supplied in parallel by blood from a central (systemic blood) compartment. Distances and relative volumes were calculated by applying the formula for the volume of a sphere (i.e., $V = 4\pi r^3/3$) for both the injected formulation and the prostate gland. It was also assumed that the formulation was positioned in the center of the selected region of the prostate gland. A schematic depiction of the six shells representing the PT compartments and the centrally positioned depot is shown in Figure 2B. The volumes and areas of the PT compartments, the mean distances between the PT compartments, and the mean distances from the respective PT compartment to the depot were then calculated on the basis of the thickness of the shells. The volume of blood within the human prostate gland was assumed to be 1.5% of the total volume of the prostate and was calculated as 0.72 mL.[27] The volume of the PT was not corrected accordingly, as the volume of blood was assumed negligible. The overall rate of prostatic blood flow (67 mL min^{-1}) and the vascular area (3230 cm^2) were calculated by adopting a blood perfusion rate of 0.97 mL min^{-1} per mL of tissue and a vascular surface density of 67 cm^2 mL^{-1}.[27−30] The volume of the prostate blood compartment, the rate of perfusion, and the surface area of each prostate compartment were then calculated from the volume fraction of each prostate compartment. The product of permeability and surface area is similar for estimates in tumors and normal tissue because the reduced vessel surface area in high-grade cancers is compensated for by increased blood flow and vessel wall permeability.[30,31] The volumes of the tumors are also usually low (<1 mL or 5−10% of the total prostate volume) at this stage of localized prostate cancer, justifying the assumption that the local disposition kinetics of 2-HOF are mainly affected by nontumor tissue. The physiological data for the PT used in the semi-PBBP model A are summarized in Table 1.

Diffusion Drug Clearances. The description of the flux of 2-HOF in the prostate was based on a multicellular layer diffusion coefficient (D_{MCL}). The D_{MCL} for 2-HOF was estimated as 1.8×10^{-6} cm^2 s^{-1} by applying eq 5[32]

$$\log(D_{MCL}) = C - [a\log(M_w)] + f(\log P) \quad (5)$$

where

$$f(\log P) = \frac{\alpha}{1 + e^{-(\log P - \beta)/\gamma}}$$

and where log P is the octanol−water partition coefficient, M_w is the molar mass (292.1 g mol^{-1}), $C = -5.6$, $a = 0.5$, $\alpha = 1.2$, $\beta = 0.7$, and $\gamma = 0.6$. Log P was estimated as 2.1 using ALOGPS2.1 based on the chemical structure of 2-HOF, described by the simplified molecular-input line-entry system (CC(C)(C(=O)NC1=CC(=C(C=C1)[N+](=O)[O−])-C(F)(F)F)O).[33]

The flux of 2-HOF between the prostate compartments was then modeled using a one-dimensional diffusion approximation, expressed by the diffusion clearance (CL_D) parameter. CL_D was calculated from eq 6 using the estimated D_{MCL}, the mean distance between the compartments (PL) and the area over which the mass transport took place (Ar)

$$CL_D = \frac{Ar \times D_{MCL}}{PL} \tag{6}$$

The values for Ar and L that were used to calculate CL_D between the tissues are listed in Table 1. The CL_D of 2-HOF between the PT and blood compartments was calculated using the vessel surface area and the distance to the blood compartment, arranged so that each blood compartment was centralized in each PT compartment, giving a distance of half the general tissue shell thickness (0.1 cm). This approach is justified by the similarities between normal and tumor tissues regarding the product of permeability and surface area.[30,31] The transmembrane transport mechanism was assumed to be dominated by passive diffusion for this rather small, lipophilic drug molecule (M_W = 292.1, log P = 2.1, PSA=75).[34] The CL_D values used for the flux of 2-HOF in PT in the semi-PBBP model are summarized in Table 2.

A one-compartment model including volume of distribution (V_d) and systemic elimination clearance (CL_{elim}) was used to describe the PK of 2-HOF in plasma. The V_d (expressed in mL) of 2-HOF in humans was estimated from previous in-house preclinical intravenous studies in rat (2100 mL/kg, weight 350 g) and dog (1800 mL/kg, weight 30 kg), using eq 7 and allometric scaling[35]

$$\log(V_d) = 0.07714\log(V_{d,rat})\log(V_{d,dog}) + 0.5147\log(V_{d,dog}) + 0.5860 \tag{7}$$

Table 2. Diffusion Clearances, CL_D, Used in the Semi-PBBP Model to Represent the Flux of 2-HOF in the Prostate[a]

prostate compartment	CL_{DbPT} (ml min^{-1}) × 10^3	CL_{DPT} (ml min^{-1}) × 10^3
1	100	9.1
2	140	13
3	190	17
4	250	21
5	320	19
6	760	

[a] CL_{DbPT} and CL_{DPT} correspond to the tissue-to-blood and the tissue-to-tissue diffusion clearances for each prostate compartment, respectively.

For the simulations of 2-HOF PK after oral administration, an intestinal absorption rate (v_{abs}) into the central compartment was modeled as a first-order process described by an absorption rate constant that was set at 0.693 h^{-1}, representing an absorption half-life of 1 h.

The average plasma concentration ($C_{ss,av}$) following oral administration of 250 mg three times daily (TID) was calculated using eq 8

$$C_{ss,av} = \frac{F \times \text{dose}}{CL_{elim} \times \tau} \tag{8}$$

where F is the bioavailability and τ is the dosage interval. The fractions of unbound 2-HOF in plasma (fu_p) and prostate tissue were set as 0.05 and 1, respectively.

Mass Transport Equations Implemented in the Semi-PBBP Model for Intraprostatic Drug Delivery. The following basic assumptions were used in this study: (i) that each compartment was well stirred, i.e. there were no concentration gradients within any of the compartments; (ii) that there was instant equilibration within each compartment, and that the concentrations of unbound 2-HOF were the same in the tissue and blood compartments; (iii) that only free (unbound to e.g. plasma protein) drug was allowed to transit between compartments; and (iv) that the concentrations in the target tissue were pharmacologically relevant.

Model Structure. The concentration of 2-HOF in the prostate tissue compartment adjacent to the MR formulation (PT1) was described by eq 9

$$\frac{dC_{PT1}}{dt} = \frac{(CL_{DPT2} \times (C_{PT2} - C_{PT1})) + (CL_{DbPT1} \times ((C_{bPT1} \times fu_p) - C_{PT1})) + v_{release}}{V_{PT1}} \tag{9}$$

where C_{PT1} is the concentration of 2-HOF in PT1, CL_{D1} is the diffusion clearance to prostate tissue in compartment 2 (PT2), CL_{DbPT1} is the diffusion clearance to the connected prostate blood compartment, V_{PT1} is the volume of PT1 and $v_{release}$ is the rate of drug release from the depot. The subscript b denotes the blood compartment.

The concentration of 2-HOF in prostate tissue compartments two to five (PT2-PT5) was described by eq 10

$$\frac{dC_{PTn}}{dt} = \frac{(CL_{DPTn+1} \times (C_{PTn+1} - C_{PTn})) + (CL_{Dn-1} \times (C_{PTn-1} - C_{PTn})) + (CL_{DbPTn} \times ((C_{bPTn} \times fu_p) - C_{PTn}))}{V_{PTn}} \tag{10}$$

where C is the concentration of 2-HOF, CL_{DPTn+1} is the diffusion clearance to the next prostate compartment, CL_{DPTn-1} is the diffusion clearance back to the previous prostate compartment, CL_{DbPTn} is the diffusion clearance to the connected prostate blood

compartment, and V is the volume of the compartment. PTn denotes prostate tissue compartment n and $bPTn$ denotes the blood compartment linked to PTn.

The concentration of 2-HOF in PT compartment six (PT6) was described by eq 11

$$\frac{dC_{PT6}}{dt} = \frac{(CL_{D5} \times (C_{PT5} - C_{PT6})) + (CL_{DbPT6} \times ((C_{bPT6} \times fu_p) - C_{PT6}))}{V_{PT6}} \quad (11)$$

where CL_{DPT5} is the diffusion clearance from PT6 to PT5, and CL_{DbPT6} is the diffusion clearance to the connected prostate blood compartment ($bPT6$).

The concentration of 2-HOF in prostate blood compartment n was modeled by eq 12

$$\frac{dC_{bPTn}}{dt} = \frac{(CL_{DbPTn} \times (C_{Pn} - (C_{bPTn} \times fu_p))) + (Q_{bPTn} \times (C_{central} - C_{bPTn})}{V_{bPTn}} \quad (12)$$

where C_{bPTn} is the concentration of 2-HOF in prostate blood compartment n, Q is the rate of blood flow, CL_{DbPT} is the diffusion clearance to the connected PT compartment, $C_{central}$ is the concentration of 2-HOF in the central compartment, and V is the compartment volume. $bPTn$ denotes the observed blood compartment and PTn denotes the PT compartment linked to $bPTn$.

The concentration of 2-HOF in the central compartment was modeled according to eq 13

$$\frac{dC_{central}}{dt} = \frac{\sum (Q_{bPTn} \times (C_{bPTn} - C_{central})) - (CL_{elim} \times C_{central}) + v_{abs}}{V_d} \quad (13)$$

The concentration of unbound 2-HOF in the central compartment ($C_{u.central}$) was calculated as $C_{central} \times fu_p$.

Semi-PBBP Model Structure B. The prostate gland in model structure B was described by one tissue compartment and one vascular compartment only. This simplification of model structure A was utilized for estimation of parameters describing the release of 2-HOF from the parenteral MR formulation and also to simulate the potential biophysical consequences of variations in the dissemination of the total dose of 2-HOF through the prostate tissue.

The outcomes of the two models (A and B) were compared. The concentration−time profiles for 2-HOF in the central compartment, that is, blood, were identical (R^2 = 1.000).

Equations 14−16 were used for model structure B. Equation 14 was used to describe the concentration of 2-HOF in the PT (C_{PT})

$$\frac{dC_{PT}}{dt} = \frac{CL_D \times ((C_{bP} \times fu_p) - C_{PT}) + v_{release}}{V_{PT}} \quad (14)$$

where C_{bPT} is the concentration of 2-HOF in prostatic blood, CL_D is the diffusion clearance between prostate tissue and prostate blood, and V_{PT} is the volume of the prostate, as in eq 6.

The concentration of 2-HOF in prostatic blood was described by eq 15

$$\frac{dC_{bPT}}{dt} = \frac{CL_D \times (C_{PT} - (C_{bPT} \times fu_p)) + (Q_P \times (C_{central} - C_{bPT})}{V_{bP}} \quad (15)$$

where Q_P is the rate of prostatic blood flow and V_{bP} is the volume of the prostate blood.

The concentration of 2-HOF in the central compartment was described by eq 16

$$\frac{dC_{central}}{dt} = \frac{(Q_P \times (C_{bPT} - C_{central}) - (CL_{elim} \times C_{central})}{V_d} \quad (16)$$

Parameter Estimations. *In Vitro Release of 2-HOF from the Depot Formulation.* The drug release-related parameters were estimated by fitting the experimental in vitro release-time profiles to the models described in eqs 3 and 4. The main parameters estimated were the various release-rate constants (k). The release model that included a third release mechanism (eq 4) was also used to estimate the fractions of 2-HOF allocated to the porous-unbound and porous-bound parts. The sum of these two fractions was always 57% of the total 2-HOF content.

In Vivo Release of 2-HOF from the Injected Depot Formulation. The mechanisms of the release of 2-HOF from the MR formulation in the in vivo analysis were modeled using the results acquired in the in vitro analysis. The parameters describing the release of 2-HOF from the depot in vivo and the CL_{elim} were estimated using model structure B by fitting the concentration in the plasma compartment to the observed plasma concentration−time profile. The mean dose of 2-HOF administered as Liproca Depot into one lobe of the peripheral zone in the clinical study (720 mg) was used in the estimations. The estimated parameters related to the depot release and in vivo disposition were used in subsequent simulations.

Simulations. *Sensitivity to Estimated Parameters.* Sensitivity simulations were carried out using the model structure B to evaluate the impact of each estimated parameter on the plasma concentration−time profile. Thus, the estimated values of k, CL_{elim}, and fraction of W allocated to the unbound and bound fractions of the porous part of the composition were varied and the impact on the result was observed. The impact of a 2-fold reduction and increase in release constants for the bound porous and nonporous material, respectively, and CL_{elim} were investigated. Also, the estimated fraction allocated to the readily available (unbound) fraction of the porous granules, that is, the unintended burst dose, was investigated at a value of zero and at a 2-fold increase.

Penetration of 2-HOF into Prostate Gland Tissue. The concentration−time profile of 2-HOF in the PT and its

Table 3. Estimated Parameters, Release Rate Constants, and Amounts of 2-HOF As Percent of the Dose Related to Each Release Process, for Modeling the in Vitro Release of 2-HOF from Liproca Depot[a]

release component	two-phase model (eq 3)			three-phase model (eq 4)		
	% of amount	k ($\mu g^{1/3}$ day^{-1})	k (day^{-1})	% of amount	k ($\mu g^{1/3}$ day^{-1})	k (day^{-1})
nonporous	43	0.30 (3.3)	0.010	43	0.35 (3.3)	0.012
porous[b]	57	1.25 (3.3)	0.039			
porous bound[c]				33 (3.6)	0.57 (5.0)	0.021
porous unbound[c] (unintended burst dose)				24 (3.6)	3.2 (2.0)	0.13
model performance	AIC = 1650, SSR = 3.3×10^8			AIC = −302, SSR = 0.35×10^8		

[a]For the two-phase analysis, rate constants were estimated and the percentage of the dose in each release component was based on the composition of the formulation. Release rate constants, in units $\mu g^{1/3}$ day^{-1}, are also displayed normalized to amount$^{1/3}$, unit day^{-1}. Estimated values are presented with CV% within brackets. [b]Adopted in the 2-phase model (eq 3). [c]Adopted in the 3-phase model (eq 4).

dependence on the diffusion distance from the depot was simulated with model structure A at single doses of 720, 1560, 2500, and 3500 mg. The model's sensitivity to changes in CL_D and prostatic blood flow was also investigated to measure its robustness to changes in input data and the effects of vascularization. The sensitivity to changes in CL_D was investigated by changing the relationship between the tissue-to-blood CL_D (CL_{DbPT}) and tissue-to-tissue CL_D (CL_{DPT}) by increasing or decreasing the CL_{DbPT} by a factor of 2. The effect of changes in blood flow was investigated by changing the total tissue perfusion rate to 0.34 mL min^{-1} per mL PT, which has been reported for healthy patients.[27]

Simulation of Dose Planning and Tissue Distribution for the Parenteral Formulation. It seemed reasonable to assume that increasing the dose and increasing the dissemination or spread of the formulation through the tissue will improve the exposure of the prostate gland to 2-HOF. These aspects were investigated by simulations using model structure B for the minimum (400 mg), mean (720 mg), and maximum (1560 mg) doses administered in the clinical study as well as for higher doses of 2500, 3500, and 4500 mg. It was recognized that 2-HOF had been disseminated through the prostate gland to a certain degree in the clinical study, according to the clinical protocol. To investigate the potential effect of increasing the spread of the formulation, simulations were performed by doubling the effective area that the formulation reached. This increase in the effective area is the equivalent of one big spherical unit being dispersed into eight smaller individual spherical units of equal size. The system was assumed to be unaltered by the treatment (i.e., no changes to the in vivo release mechanisms, formulation composition, or physiological response). Thus, to investigate the implications of spreading the same dose, eq 4 was multiplied by two.

Repeated Oral Administration of Flutamide. A dosage of 250 mg flutamide TID was simulated using model structure B. The $C_{ss,av}$ for 2-HOF was calculated using eq 8, assuming that the complete dose of flutamide reached the systemic circulation and was metabolized to 2-HOF, that is, that the dose of 2-HOF was equal to the dose of flutamide. This exercise was carried out in order to facilitate a comparison of 2-HOF exposure between the conventional oral route of administration and the local intraprostatic depot route. A predictive comparison between simulated plasma and prostate concentrations of 2-HOF following local single-dose administration of 2-HOF (Liproca Depot: 720, 1560, 2500, and 3500 mg) and repeated oral administration of flutamide (250 mg TID) was also carried out using model structure A.

In Vitro–In Vivo Correlation. The rate of drug release in vitro was correlated with that in vivo by relating the normalized release constants for each component in the formulation, that is, porous and nonporous. The constants were normalized to the cubic root of the initial amount of 2-HOF ($W^{1/3}$) to acquire mass-normalized rate constants ($k/W^{1/3}$) with units day^{-1}. The normalized rate constants were compared in the IVIVC. The amounts and rate constants related to respective mechanisms, that is, porous and nonporous, were acquired from the in vitro and in vivo analyses. The IVIVC was also simulated using model structure B and scaled in vitro release parameters for an intraprostatic 2-HOF dose of 720 mg as Liproca Depot.

Data Analysis. Akaike information criteria (AIC), sum of squared residuals (SRR), visual examination, and the precision of parameter estimation were investigated to evaluate and compare the goodness of fit for the different models. All analyses of kinetic data were performed (weighted $1/\hat{y}^2$) using WinNonlin Professional software V6.3 (Pharsight Corp., CA). Simulations were performed with Berkeley Madonna software v8.3.18 (University of California, Berkley, CA, U. S. A.).

RESULTS

In Vitro Release of 2-HOF. The results from the in vitro investigation are summarized in Table 3. Observations from the in vitro experiment and simulated model curve corresponding to the two-phase release and the three-phase release models are shown in Figure 3. The model with three simultaneous release mechanisms described the in vitro release significantly better than the two-phase model (two-phase AIC = 1650, SSR = 3.3×10^8, three-phase AIC = −302, SSR = 0.35×10^8). The estimated in vitro release rate constants were: $k_{p-ub} = 3.2$ $\mu g^{1/3}$ day^{-1}, $k_{p-b} = 0.57$ $\mu g^{1/3}$ day^{-1}, and $k_{np} = 0.35$ $\mu g^{1/3}$ day^{-1}. The readily available fraction, that is, the unbound burst dose of 2-HOF from the porous part of the MR formulation, was estimated to be 24% of the total dose with the three-phase model in vitro.

In Vivo Release of 2-HOF. *Depot release and description of plasma concentration–time profile for 2-HOF.* There was a high correlation between the plasma compartment kinetics and the observed plasma concentration–time profiles for 2-HOF, fitting the three-component (eq 4) release model, based on the in vitro investigation for drug release from the depot (Figure 4). In vivo release parameters are listed in Table 4. The estimated release rate constants were: $k_{p-ub} = 15$ $\mu g^{1/3}$ day^{-1}, $k_{p-b} = 7.9$ $\mu g^{1/3}$ day^{-1}, and $k_{np} = 1.7$ $\mu g^{1/3}$ day^{-1}. The fraction of unbound 2-HOF in the porous part of the formulation (i.e., the burst dose) was estimated to be 3% of the total dose in vivo. CL_{elim} was estimated as 630 L day^{-1} and the V_d used in the estimations and simulations was predicted, by allometric scaling, to be 1.3 L kg^{-1}. A plot of the observations from the clinical study and the model fit is shown in Figure 4.

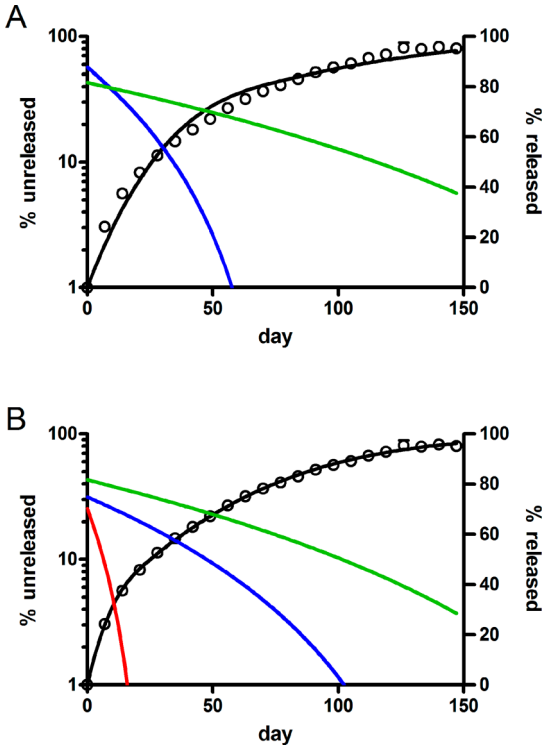

Figure 3. Observed in vitro release of 2-HOF (open circles) displayed as means ± SD (n = 4), and the model fit (black) of total % of 2-HOF released. Colored lines represents the percent unreleased from the respective formulation component (red = porous unbound, blue = porous bound, green = nonporous). (A) Release model described by two release mechanisms (eq 3). (B) Release model described by three release mechanisms (eq 4).

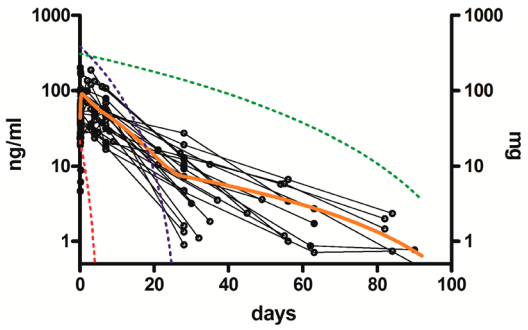

Figure 4. Individual plasma concentration−time profiles for 2-HOF from the clinical study in patients with local prostate cancer (T1-T2) (connected black circles) and the model fit (orange solid line) using Model structure B. Colored dotted lines represent the amount of 2-HOF still to be released from the respective formulation component (red = porous unbound, blue = porous bound, green = nonporous).

Table 4. Estimated Parameters for the in Vivo Release of 2-HOF from Liproca® Depot[a]

release component	% of amount	k ($\mu g^{1/3}$ day^{-1})	k (day^{-1})
nonporous	43	1.7	0.025
porous bound	54	7.9	0.11
porous unbound	3	15	0.54

[a]Release rate constants, in units of $\mu g^{1/3}$ day^{-1}, are also displayed normalized to amount$^{1/3}$ with the unit of day^{-1}.

Simulations. *Sensitivity Simulations.* The results from the sensitivity simulations, using changes to the estimated parameters from the in vivo analysis, are presented in Figure 5. The terminal half-life of 2-HOF in plasma was dependent on its rate of release from the dense nonporous granules, whereas the area under the plasma concentration−time curve (exposure, AUC) for 2-HOF was also dependent on CL_{elim}. The initial (0−2 days) increase in plasma concentrations was partly determined by the fraction of unbound 2-HOF in the porous granules at the exposed surfaces. However, in relation to the two main release components, the fraction of unbound 2-HOF in the porous granules, that is, unintended burst part, had negligible influence on the overall plasma profile. The initial (0−2 days) and midperiod (2−20 days) plasma profiles were dominated by the porous composition, whereas the extended profile (20−92 days) was determined by the dense material in the depot formulation.

Prostate Tissue Concentration and Tissue Penetration of 2-HOF. The penetration of 2-HOF in the PT following a single dose of the parenteral MR formulation was simulated using model structure A. The model was capable of simulating the PT concentration (C_{PT}) in relation to the distance to the local depot over time (spatiotemporal) (Figure 6). At pseudo-equilibrium, the $C_{PT}/C_{u.central}$ ratios for the PT compartments PT1-PT6 (mean distance to depot formulation in brackets) were as follows: PT1 39000 (1 mm), PT2 1200 (3 mm), PT3 36 (5 mm), PT4 2.1 (7 mm), PT5 1.0 (9 mm), and PT6 1.0 (12 mm). For the whole PT this was equivalent to an average $C_{PT}/C_{u.central}$ ratio of 2400. This corresponds to a total concentration of 2-HOF in PT that is 120 times higher than that in plasma. This demonstrates that the targeting and accumulation of 2-HOF is potentially significant over an area of 5 mm in each direction from the depot surface. Each discrete unit of the formulation will consequently affect a total axial length of 10 mm of tissue throughout the dosage interval. The tissue penetration of 2-HOF was dependent on the relationship between CL_{DPT} and CL_{DbPT}, as displayed in Figure 7. As CL_D is compartment-specific (dependent on area and length), the CL_{DbPT}/CL_{DPT} ratio is given as a range. The simulated reduction of prostatic blood flow from 0.97 mL min^{-1} per mL PT to a healthy level, 0.34 mL min^{-1} per mL PT, had no impact on the PT tissue penetration or plasma concentration−time profile of 2-HOF.[27−30]

Impact of Dose and Dispersion of the MR Formulation on the Release and Plasma PK of 2-HOF. The predicted effects of variations in the dose and extent of dissemination of the MR formulation are shown in Figure 8. When the same parenteral dose was distributed further throughout the prostate gland, the total amount of released 2-HOF per time was increased because of the larger surface area available for drug release from the depot formulation. As a result, C_{max} in plasma and tissue increased and the terminal plasma half-life of 2-HOF was reduced. Increased distribution also increased the fraction of the PT that was close to the depot. For instance, when applying the geometry of a sphere, if the formulation is kept roughly as one unit (i.e., minimal dissemination), approximately 20% of the PT will be within 5 mm of the depot, which should easily cover the volume of most tumors of about 0.5−1 mL in this patient category.[36] This percentage would theoretically increase to approximately 63% if the same volume of the formulation is divided into 8 units. This supports a dosage strategy that, with the assistance of modern imaging techniques, could provide highly precise tumor-directed therapy.

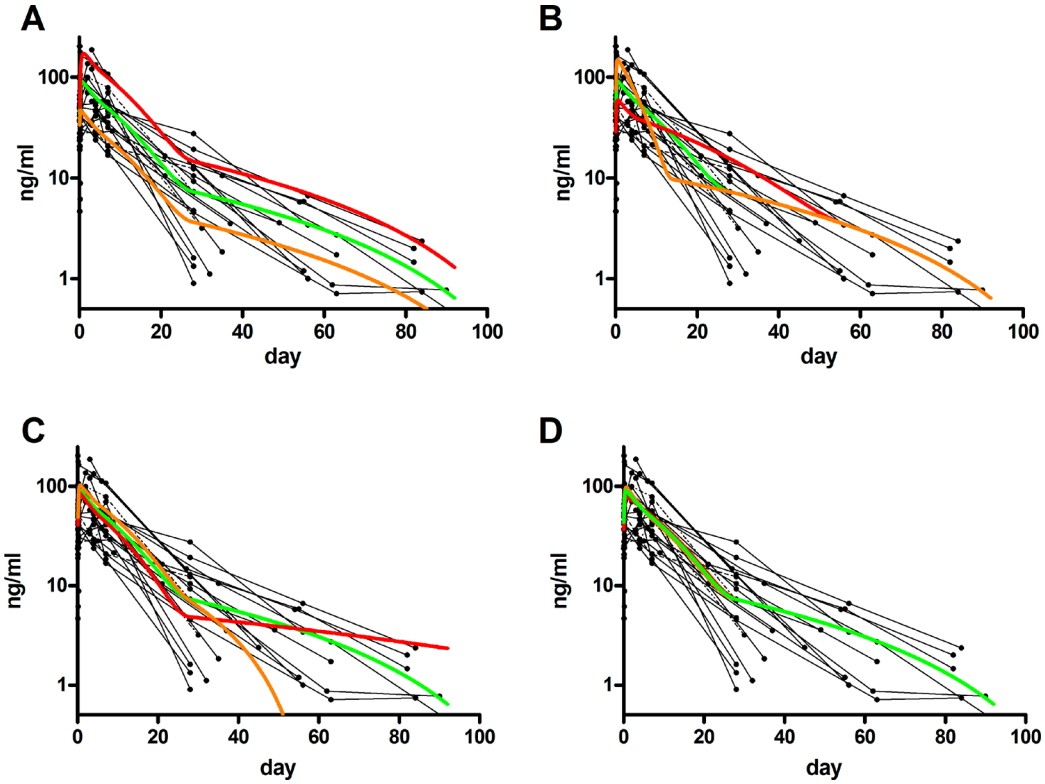

Figure 5. Sensitivity plots simulating the impact on the systemic (blood) 2-HOF concentration–time profiles of changes to (A) the systemic elimination clearance (CL_{elim}), (B) the release rate from the porous composition containing bound drug (corresponding to 54% of total dose), (C) the release rate from the dense nonporous composition (corresponding to 43% of total dose), and (D) the amount of available unbound 2-HOF in the porous composition (corresponding to 3% of total dose). The graph shows individual plasma concentration–time profiles for 2-HOF from the clinical study (connected black dots) and the simulated concentrations in the central compartment (solid lines). Estimated parameters from the in vivo analysis were used as reference (green). Simulations for increases (double the values for (A) CL_{elim}, (B) k_{p-b}, (C) k_{np}, and (D) the amount of unbound drug in the porous compartment; shown in orange) and decreases (half the values for (A) CL_{elim}, (B) k_{p-b}, and (C) k_{np}, and (D) zero unbound drug in the porous compartment; shown in red) in the reference input data are shown in the plots.

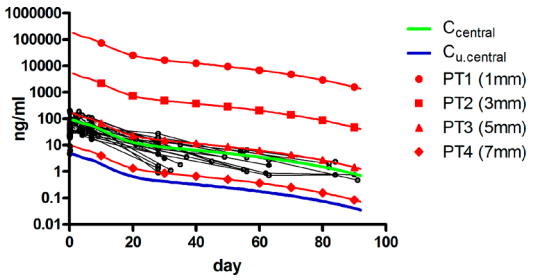

Figure 6. Individual plasma concentration–time profiles for 2-HOF from the clinical study in patients with local prostate cancer (T1-T2) (connected black circles) and simulated concentration–time profiles for total (green) and unbound (blue) 2-HOF in the central compartment and for 2-HOF in the prostate tissue compartments (PT; red) PT1 (dots), PT2 (squares), PT3 (triangles), PT4 (diamonds), with the mean distance to the depot formulation shown in millimeters. The concentrations in PT5 and PT6 were the same as the concentration of unbound 2-HOF in the systemic plasma and these values were thus excluded from the plot.

2-HOF Plasma Concentrations after Repeated Oral Administration of Flutamide (250 mg TID). The simulated plasma concentration–time profile for 2-HOF after 250 mg oral flutamide TID (total daily dose of 750 mg for 5 days) is shown in Figure 9. The calculated $C_{ss,av}$ after oral administration was 1180 ng mL^{-1}, which is similar to previously reported 2-HOF concentrations after oral administration of flutamide 250 mg TID (1629 ± 586 ng mL^{-1}).[37] After oral administration, the concentration of 2-HOF in the PT was equivalent to the concentration of unbound 2-HOF in plasma (i.e., the systemic concentration). The comparison between simulated systemic plasma and prostate concentrations of 2-HOF following a local single dose of Liproca Depot (720, 1560, 2500, and 3500 mg) and repeated oral doses of flutamide 250 mg TID is shown in Figure 10.

In Vitro–In Vivo Correlations. The comparison of the normalized release rate constants ($k/W^{1/3}$) acquired from in vitro and in vivo analyses is shown in Table 5. Figure 11 shows the simulated in vivo plasma concentration–time profile using the estimated in vitro release parameters from the three-phase release model, scaled to a clinical dose of 720 mg, using the semi-PBBP model structure B, and PK parameters estimated from the in vivo study. Although the simulated plasma profile showed dissimilarities to the estimated plasma profile, especially in the early to middle stages, it corresponded reasonably well with observations. This was mainly a consequence of the acceptable correlation acquired for the nonporous slow release component in the formulation. Despite the discrepancies, this comparison demonstrated that a reasonably accurate, direct IVIVC is possible using the suggested release approach and in vitro methodology. The results suggest that the applied in vitro method and the theoretical approach for the release can be used in assessing the clinical performance of this parenteral MR formulation.

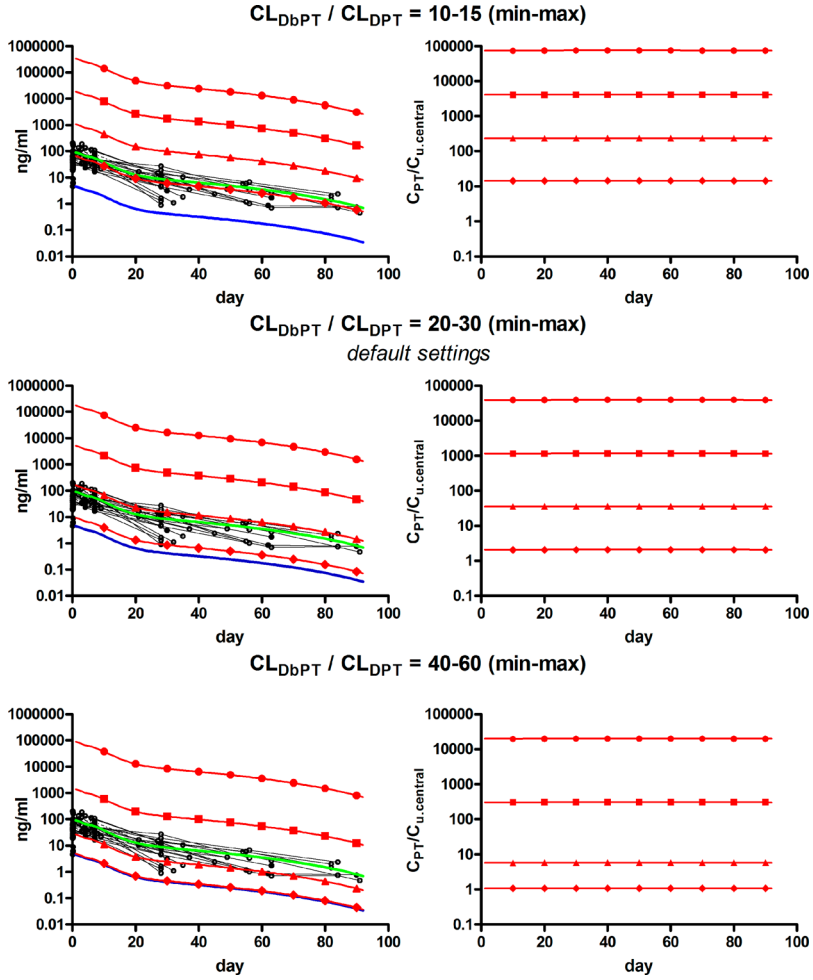

Figure 7. Impact of the relationship between the tissue-to-blood (CL_{DbPT}) and tissue-to-tissue (CL_{DPT}) intraprostatic diffusion clearances on the 2-HOF prostate tissue (PT) concentrations. The graphs show the individual plasma concentration−time profiles for 2-HOF from the clinical study (connected black squares) and simulated concentration−time profiles for total (green) and unbound (blue) 2-HOF in the central compartment and for 2-HOF in the PT compartments (red) PT1 (dots), PT2 (squares), PT3 (triangles), PT4 (diamonds), at mean distances from the depot formulation of 1, 3, 5, and 7 mm, respectively. The concentrations in PT5 and PT6 were the same as the concentration of unbound 2-HOF in the systemic plasma and these values were thus excluded from the plots. For each setting, the 2-HOF tissue accumulation is also shown as the concentration in the PT (C_{PT}) divided by the concentration of unbound 2-HOF in the central compartment ($C_{u.central}$).

■ DISCUSSION

A semi-PBBP model was developed to investigate tissue concentrations and the spatiotemporal distribution of 2-HOF in the prostate gland after intraprostatic single-dose delivery of an MR formulation. The parenteral MR formulation was microstructurally designed to provide fast and slow rates of release of 2-HOF from the porous and dense nonporous parts of the formulation, respectively. In the model analysis, the in vivo release of 2-HOF agreed well with two-phase release characteristics. The semi-PBBP model was based on plasma concentration−time data for 2-HOF obtained from a phase II study in 24 patients with localized PC (T1-T2), in which a single mean dose of 720 mg 2-HOF in the depot formulation was injected by TRUS into one lobe of the prostate gland.[16] Simulations using the semi-PBBP model produced realistic prostate concentration−time profiles and spatiotemporal distributions of 2-HOF in the PT. In addition, plasma PK profiles after oral administration were replicable. Finally, an IVIVC of the release rates of 2-HOF was partially established.

The reformulated Noyes−Whitney equation (eq 1), which describes the direct correlation between the release rate and the amount of API in the dose, accurately described the in vitro drug release profile. The three-phase release model (eq 4), determined to be the most appropriate one from the in vitro investigation, was used to describe drug release in the PBBP model, which was then used to estimate the in vivo release rate. The IVIVC subsequently showed a reasonably good correlation for the nonporous (dense) slow release part of the formulation. No direct correlation was found between in vitro and in vivo results for release from the porous part (i.e., the estimated release rate constants and the fraction of unintended burst of unbound drug from the porous part were both different). There are several potential reasons for these discrepancies. One may be differences in the overall shape of the depot formulations in the in vitro and in vivo investigations. The in vitro study was performed with roughly hemispherical lumps of solidified formulation, with theoretically less available surface area than would be seen when dissolving the more unevenly distributed formulation occurring in vivo, when the formulation is disseminated across the prostate gland (see discussion below in relation to Figure 12). Another possible cause to the observed differences between the in vitro and in vivo characteristics

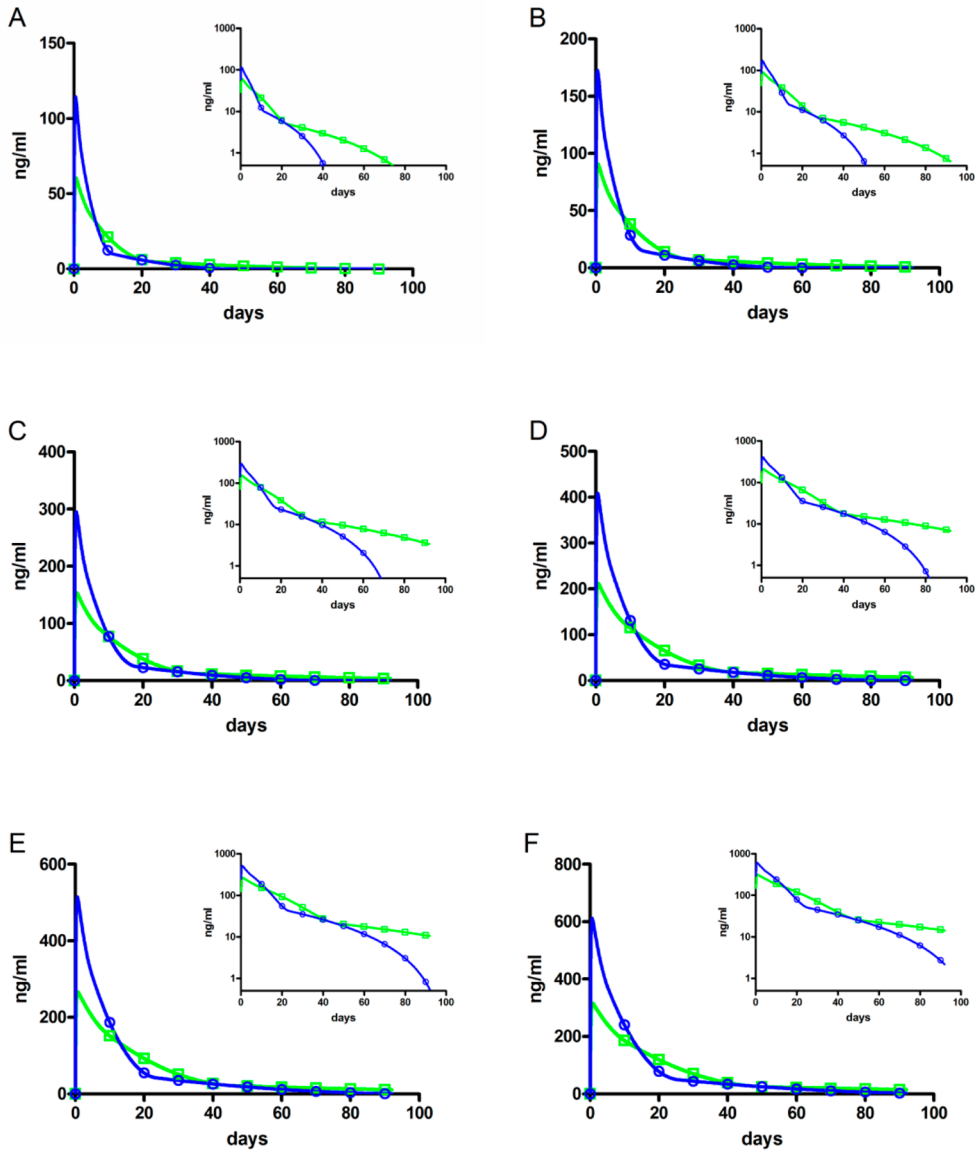

Figure 8. Simulations of the impact of dose and dissemination of the formulation on the concentration of 2-HOF in the central compartment. Simulated concentration−time profiles in the central compartment are shown for the mean dissemination seen in the clinical study (green) and the area increased by a factor of 2 (blue) after intraprostatic administration of the depot formulation containing a dose of (A) 400 mg, (B) 720 mg, (C) 1560 mg, (D) 2500 mg, (E) 3500 mg, and (F) 4500 mg. Lin−log scaled inserts of the respective plots are included.

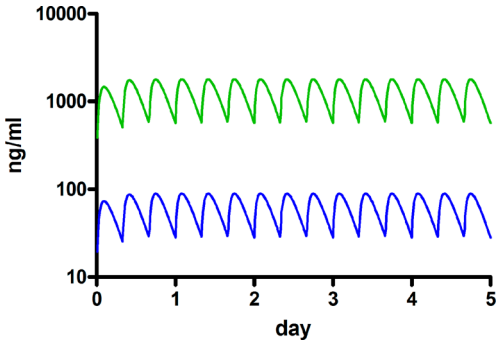

Figure 9. Simulated concentration−time profiles for total (green) and unbound (blue) 2-HOF in the central compartment (systemic plasma) during repeated oral administration of flutamide 250 mg TID, assuming that the complete dose of flutamide reached the systemic circulation as 2-HOF.

is the interaction between the formulation and the surrounding media. This seems highly plausible, considering that the release of 2-HOF from the porous part was influenced more than from the compressed dense part, which is largely embedded in (and protected by) the surrounding porous matrix. In addition, the human prostate gland has a higher capacity to maintain local sink conditions and reduce the aqueous boundary layer surrounding the formulation than the more unstirred in vitro situation. The flow of biological fluids in the PT in vivo might also affect the formulation differently from the in vitro assay setup. The potential for disintegration of the porous part of the MR formulation is increased by the mechanical forces resulting from intraorgan fluid movements and tissue contractions. One month after it was administered by intraprostatic injection in a preclinical efficacy and safety study in dogs, the MR formulation was seen to be distributed as small particles (Figure 12), which is in contrast to the in vitro setup where a

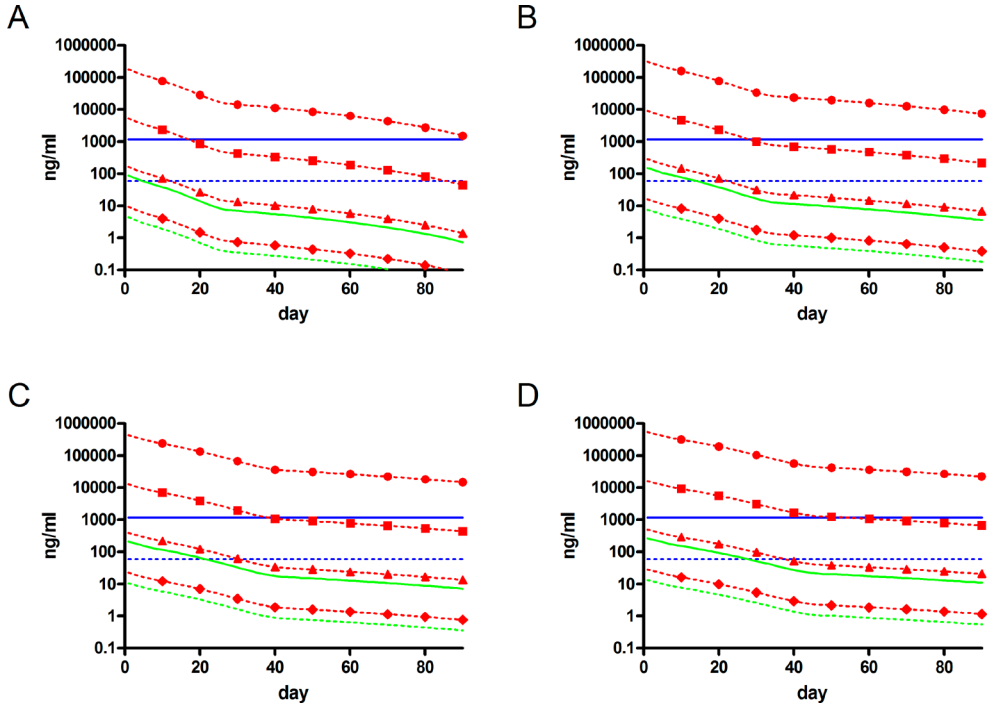

Figure 10. Simulated concentration−time profiles for 2-HOF following a single intraprostatic dose of the depot formulation (720 mg (A), 1560 mg (B), 2500 mg (C), and 3500 mg (D)) and repeated oral 250 mg doses of flutamide TID. The blue lines represent average plasma concentrations after oral administration and the green lines represent plasma concentrations after administration of the intraprostatic depot formulation. The red lines show the concentrations in prostate tissue (PT) compartments PT1 (dots), PT2 (squares), PT3 (triangles), and PT4 (diamonds), at mean distances of 1, 3, 5, and 7 mm from the depot formulation, respectively. Solid and dotted lines represent total and unbound 2-HOF concentrations, respectively.

Table 5. Comparison of the Area-Normalized Release Rate Constants, $k/W^{1/3}$, Acquired from the in Vitro, $k_{\text{in vitro}}$, and in Vivo, $k_{\text{in vivo}}$, Analyses Carried out Using the Three-Phase Release Model[a]

formulation component	$k_{\text{in vitro}}/k_{\text{in vivo}}$
nonporous	0.47
porous, bound drug	0.20
porous, unbound drug	0.24

[a]Equation 4.

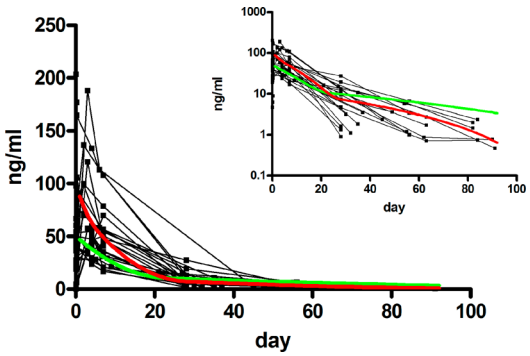

Figure 11. Simulated plasma concentration−time profile for 2-HOF obtained using release parameters acquired from the in vitro experiments (green line). Individual plasma concentration−time profiles for 2-HOF from the clinical study (connected black squares) and the model fit (red line) using model structure B are also shown. A lin−log scaled insert is included.

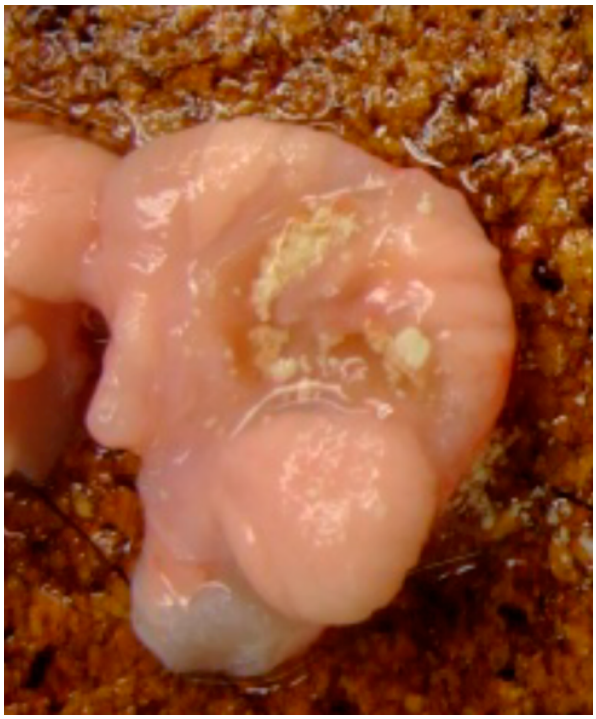

Figure 12. Resected prostate gland that was removed 12 weeks after administration of the parenteral MR formulation during a GLP toxicological study in dogs.[12]

single unit of the formulation was investigated. It is also possible that the observed discrepancy between in vitro and in vivo behavior is a result of a more dense calcium sulfate-based matrix formed by solidification in moisture (in vivo), creating stronger structures than when solidification occurs in

air (in vitro). Because the fraction of unbound drug (burst dose) only represented about 3% of the total released dose in vivo, in comparison to 24% in vitro, it appears that the in vivo release of 2-HOF was more than 95% controlled by the two designed release compartments in the MR formulation. The immediately available fraction in the in vivo scenario is hence probably mostly represented by 2-HOF located on the outer surface of the formulation. It is also notable that the amount released as a nondeliberate burst in vivo was lower in this MR parenteral formulation than in other parenteral formulations.[23,24] From both efficacy and safety perspectives, the demonstrated IVIVC for the slow release of drug from the dense nonporous part of the MR formulation is very encouraging for future pharmaceutical and clinical development.

The sensitivity evaluations of the model (Figure 5) indicated that both designed release components of the formulation were required to reach the targeted local concentration−time profile (a fast onset of action and prolonged 2-HOF exposure over time). The increase in plasma C_{max} and the extent of systemic exposure during the first weeks were dominated by the release of 2-HOF from the porous part, whereas the prolonged exposure and terminal half-life were determined by release from the nonporous part. Changes in the CL_{elim} had a direct effect on the exposure of plasma to 2-HOF, as expected, but not on the terminal half-life. This was because the release rate from the formulation was considerably slower than the rate of blood flow through the prostate gland. The extent of tissue penetration and the concentration gradient of 2-HOF inside the prostate gland were sensitive to the CL_D values within the tissue and between the tissue and the blood. This is an important consideration, in that these values determine the mean distance that a 2-HOF molecule will diffuse in the tissue before it distributes to a blood vessel. It should be noted that the mass transport of 2-HOF in the PT was modeled by a one-dimensional diffusion approximation. As these calculations were based on several assumptions, both theoretical and physiological, some degree of caution is recommended regarding absolute numbers and concentration levels.

At distances of 3 and 5 mm from the depot formulation, the 2-HOF PT concentrations were predicted to be 1200 times and 36 times higher, respectively, than the free 2-HOF concentrations in plasma. This indicates that substantial accumulation of the API occurs in the PT at a distance of up to 5 mm from the dose unit. It has been shown that there is no (or a minimal) fibrous capsule formed around the formulation (Figure 12) that could potentially restrict drug transport.[38] It is expected that local sustained exposure to the active drug will significantly reduce the tumor volume, resulting in good cancer control without the normal high frequency of antiandrogen-related side effects.[39,40] The systemic exposure to 2-HOF over the investigated time period, after local administration of this MR formulation, was shown to be approximately 5% of the concentration reached after repeated oral administration.[37] This low systemic exposure to 2-HOF is a clear advantage with respect to minimizing the risks of systemic androgen-related adverse effects.

Dissemination of the formulation through the PT will, according to the theoretical release-distribution model, increase both the volume of the prostate gland exposed to the drug and the total rate of release (of the complete dose). This was shown in the simulations not only as an initial increase in both plasma and prostate concentrations but also as a decrease in the terminal half-life. This implies that the administration procedure per se might have an impact on the overall release rate but not on the local 2-HOF release rate from each depot unit. Further investigation into the dissemination of the formulation throughout the gland is to be carried out in the clinic using a standardized procedure based on imaging guidance; a high probability of sufficient tumor exposure to 2-HOF is expected. The investigation of 2-HOF tissue penetration suggests that the depot should be located as close to the tumor tissue as possible, preferably with some degree of spreading around the tumor area as well. In the clinic, this can be attained by combining diagnostic imaging with TRUS guidance. The distribution investigation assumed that the dissemination of the formulation into the surrounding tissue was completely unaffected by the neighboring depot units. This is a very simplified view of the in vivo situation as the surrounding tissue will also receive 2-HOF from the adjacent units. As a result, the simulated tissue concentration in the dissemination investigation should be regarded as a minimum.

The delivery of 2-HOF to cells in a solid tumor is a dynamic process that is determined by the drug concentration, the duration of treatment, and the general processes involved in drug distribution (i.e., the rate of distribution of the drug through the vascular space, the rate and extent of transport across microvessel walls, the extent of carrier-mediated cellular membrane transport (influx−efflux), and the extent of diffusion through the interstitial space in the tumor tissue). The pharmacological effects of 2-HOF, which have not been included in this semi-PBBP model, will probably also affect its intraprostatic disposition. These effects, as well as clinical aspects such as treatment schedules and pretreatment to induce cell death, would need to be taken into consideration in order to fully investigate the tumor-targeting potential of this MR formulation and to maximize drug delivery to the hard-to-reach tumor cells. This semi-PBBP model and the results of the study presented here provide a basis for future investigations and evaluations.

In conclusion, the semi-PBBP model simulations show that the intraprostatic concentrations of 2-HOF are significantly higher than the systemic plasma concentrations after a single-dose intraprostatic injection of the studied MR formulation and that increased distribution of 2-HOF throughout the gland is possible with a strategic dosage plan. Accumulation of 2-HOF to a concentration at least 40 times the plasma concentration is potentially possible, at a distance of 5 mm in all directions from the depot surface; thus, each discrete unit of the formulation will expose a total PT axial length of 10 mm to the drug throughout the dosage interval. This novel parenteral MR formulation design thus offers potential for good pharmacological effect with a minimum risk of side effects for patients with local prostate cancer.

■ AUTHOR INFORMATION

Corresponding Author

*H. Lennernäs. E-mail: hans.lennernas@farmaci.uu.se. Telephone: +46 18 471 4317. Fax: +46 18 471 4223. Address: Biopharmaceutical Research Group Department of Pharmacy, Uppsala University, Box 580, SE-751 23 Uppsala, Sweden.

Notes

The authors declare the following competing financial interest(s): Niklas Axn, Hans Lennerns, Bo Lennerns and Lars-Åke Malmsten have equity interests in LIDDS AB and have acted as consultants for the company.

■ ABBREVIATIONS

2-HOF, 2-hydroxyflutamide; *A*, surface area; ADT, androgen deprivation therapy; AIC, Akaike information criteria; API, active pharmaceutical ingredient; Ar, area of mass transport; b, blood compartment; *C*, concentration; $C_{central}$, central compartment concentration; C_{PT}, prostatic tissue concentration; $C_{ss,av}$, average plasma concentration at steady state; CL, clearance; CL_D, diffusion clearance; CL_{DPT}, tissue-to-tissue diffusion clearance; CL_{DbPT}, tissue-to-blood diffusion clearance; CL_{elim}, systemic elimination clearance; *D*, diffusion constant; D_{MCL}, multicellular layer diffusion coefficient; *F*, bioavailability; fu_p, fraction of unbound 2-HOF in plasma; IVIVC, in vitro−in vivo correlation; *k*, release-rate constant; *L*, diffusion-layer thickness; LC−MS/MS, liquid chromatography coupled with tandem mass spectrometry; log *P*, octanol−water partition coefficient; MR, modified-release; M_W, molar mass; *n*, compartment n; *np*, nonporous; *p*, porous; *p-b*, porous/bound drug; PBBP, physiologically based biopharmaceutical; PC, prostate cancer; PK, pharmacokinetic(s); PL, distance between compartments; PSA, prostate-specific antigen; PT, prostate tissue; *p-ub*, porous/unbound drug; *Q*, rate of blood flow; SRR, sum of squared residuals; TID, three times a day; tot, total; TRUS, transrectal ultrasound; τ, dosage interval; *V*, volume of compartment; v_{abs}, intestinal absorption rate; V_d, volume of distribution; $v_{release}$, rate of drug release from the depot; *W*, weight of 2-HOF

■ REFERENCES

(1) American Cancer Society. *Cancer Facts & Figures 2013*; American Cancer Society, Atlanta: 2013.

(2) Sieh, W.; Lichtensztajn, D. Y.; Nelson, D. O.; Cockburn, M.; West, D. W.; Brooks, J. D.; Chang, E. T. Treatment and Mortality in Men with Localized Prostate Cancer: A Population-Based Study in California. *Open Prostate Cancer J.* **2013**, *6*, 1−9.

(3) Paller, C. J.; Antonarakis, E. S.; Eisenberger, M. A.; Carducci, M. A. Management of patients with biochemical recurrence after local therapy for prostate cancer. *Hematol. Oncol. Clin. North Am.* **2013**, *27* (6), 1205−19 viii.

(4) Widmark, A.; Klepp, O.; Solberg, A.; Damber, J. E.; Angelsen, A.; Fransson, P.; Lund, J. A.; Tasdemir, I.; Hoyer, M.; Wiklund, F.; Fossa, S. D. Scandinavian Prostate Cancer Group, S.; Swedish Association for Urological, O. Endocrine treatment, with or without radiotherapy, in locally advanced prostate cancer (SPCG-7/SFUO-3): an open randomised phase III trial. *Lancet* **2009**, *373* (9660), 301−8.

(5) Denham, J. W.; Steigler, A.; Lamb, D. S.; Joseph, D.; Turner, S.; Matthews, J.; Atkinson, C.; North, J.; Christie, D.; Spry, N. A.; Tai, K. H.; Wynne, C.; D'Este, C. Short-term neoadjuvant androgen deprivation and radiotherapy for locally advanced prostate cancer: 10-year data from the TROG 96.01 randomised trial. *Lancet Oncol.* **2011**, *12* (5), 451−9.

(6) Albertsen, P. C.; Klotz, L.; Tombal, B.; Grady, J.; Olesen, T. K.; Nilsson, J. Cardiovascular morbidity associated with gonadotropin releasing hormone agonists and an antagonist. *Eur. Urol.* **2014**, *65* (3), 565−73.

(7) Lu-Yao, G. L.; Albertsen, P. C.; Li, H.; Moore, D. F.; Shih, W.; Lin, Y.; DiPaola, R. S.; Yao, S. L. Does primary androgen-deprivation therapy delay the receipt of secondary cancer therapy for localized prostate cancer? *Eur. Urol.* **2012**, *62* (6), 966−72.

(8) McLeod, D. G.; Iversen, P.; See, W. A.; Morris, T.; Armstrong, J.; Wirth, M. P. Casodex Early Prostate Cancer Trialists, G. Bicalutamide 150 mg plus standard care vs standard care alone for early prostate cancer. *BJU Int.* **2006**, *97* (2), 247−54.

(9) McLeod, D. G.; See, W. A.; Klimberg, I.; Gleason, D.; Chodak, G.; Montie, J.; Bernstein, G.; Morris, C.; Armstrong, J. The bicalutamide 150 mg early prostate cancer program: findings of the North American trial at 7.7-year median followup. *J. Urol.* **2006**, *176* (1), 75−80.

(10) Widmark, A.; Klepp, O.; Solberg, A.; Damber, J.-E.; Angelsen, A.; Fransson, P.; Lund, J.-Å.; Tasdemir, I.; Hoyer, M.; Wiklund, F.; Fosså, S. D. Endocrine treatment, with or without radiotherapy, in locally advanced prostate cancer (SPCG-7/SFUO-3): an open randomised phase III trial. *Lancet* **2009**, *373* (9660), 301−308.

(11) Ortiz, R.; Au, J. L.; Lu, Z.; Gan, Y.; Wientjes, M. G. Biodegradable intraprostatic doxorubicin implants. *AAPS J.* **2007**, *9* (2), E241−50.

(12) *LIDDS AB, SWEDEN*; Data on file.

(13) Simard, J.; Singh, S. M.; Labrie, F. Comparison of in vitro effects of the pure antiandrogens OH-flutamide, Casodex, and nilutamide on androgen-sensitive parameters. *Urology* **1997**, *49* (4), 580−6 discussion 586−9.

(14) Li, Y.; Wang, J.; Gao, Y.; Zhu, J.; Wientjes, M. G.; Au, J. S. Relationships between Liposome Properties, Cell Membrane Binding, Intracellular Processing, and Intracellular Bioavailability. *AAPS J.* **2011**, *13* (4), 585−597.

(15) Chou, C. Y.; Huang, C. K.; Lu, K. W.; Horng, T. L.; Lin, W. L. Investigation of the spatiotemporal responses of nanoparticles in tumor tissues with a small-scale mathematical model. *PLoS One* **2013**, *8* (4), e59135.

(16) Tammela, T.; Häggman, M.; Ladjevardi, S.; Ahlström, H.; Von Below, C.; Lennernäs, B.; Tolf, A.; Weiss, J.; Wassberg, C.; Axén, N.; Lennernäs, H. Local antiandrogen therapy, a novel treatment strategy for localized prostate cancer. *Scand. J. Urol.* **2014**.

(17) Siepmann, J.; Siepmann, F. Mathematical modeling of drug delivery. *Int. J. Pharm.* **2008**, *364* (2), 328−43.

(18) Costa, P.; Sousa Lobo, J. M. Modeling and comparison of dissolution profiles. *Eur. J. Pharm. Sci.* **2001**, *13* (2), 123−33.

(19) Noyes, A. A.; Whitney, W. R. The rate of solution of solid substances in their own solutions. *J. Am. Chem. Soc.* **1897**, *19* (12), 930−934.

(20) Edwards, L. J. The Dissolution and Diffusion of Aspirin in Aqueous Media. *Trans. Faraday Soc.* **1951**, *47* (11), 1191−1210.

(21) Hixson, A. W.; Crowell, J. H. Dependence of Reaction Velocity upon surface and Agitation. *Ind. Eng. Chem.* **1931**, *23* (8), 923−931.

(22) Frenning, G. Theoretical investigation of drug release from planar matrix systems: effects of a finite dissolution rate. *J. Controlled Release* **2003**, *92* (3), 331−9.

(23) Huang, X.; Brazel, C. S. On the importance and mechanisms of burst release in matrix-controlled drug delivery systems. *J. Controlled Release* **2001**, *73* (2−3), 121−36.

(24) Martinez, M.; Rathbone, M.; Burgess, D.; Huynh, M. In vitro and in vivo considerations associated with parenteral sustained release products: a review based upon information presented and points expressed at the 2007 Controlled Release Society Annual Meeting. *J. Controlled Release* **2008**, *129* (2), 79−87.

(25) Hicks, K. O.; Pruijn, F. B.; Baguley, B. C.; Wilson, W. R. Extravascular transport of the DNA intercalator and topoisomerase poison N-[2-(Dimethylamino)ethyl]acridine-4-carboxamide (DACA): diffusion and metabolism in multicellular layers of tumor cells. *J. Pharmacol. Exp. Ther.* **2001**, *297* (3), 1088−98.

(26) Hicks, K. O.; Pruijn, F. B.; Sturman, J. R.; Denny, W. A.; Wilson, W. R. Multicellular resistance to tirapazamine is due to restricted extravascular transport: a pharmacokinetic/pharmacodynamic study in HT29 multicellular layer cultures. *Cancer Res.* **2003**, *63* (18), 5970−7.

(27) Franiel, T.; Ludemann, L.; Rudolph, B.; Rehbein, H.; Stephan, C.; Taupitz, M.; Beyersdorff, D. Prostate MR imaging: tissue characterization with pharmacokinetic volume and blood flow parameters and correlation with histologic parameters. *Radiology* **2009**, *252* (1), 101−8.

(28) Franiel, T.; Ludemann, L.; Rudolph, B.; Lutterbeck, E.; Hamm, B.; Beyersdorff, D. Differentiation of prostate cancer from normal prostate tissue: role of hotspots in pharmacokinetic MRI and histologic evaluation. *AJR, Am. J. Roentgenol.* **2010**, *194* (3), 675−81.

(29) Ludemann, L.; Prochnow, D.; Rohlfing, T.; Franiel, T.; Warmuth, C.; Taupitz, M.; Rehbein, H.; Beyersdorff, D. Simultaneous

quantification of perfusion and permeability in the prostate using dynamic contrast-enhanced magnetic resonance imaging with an inversion-prepared dual-contrast sequence. *Ann. Biomed. Eng.* **2009**, *37* (4), 749−62.

(30) Barth, P. J.; Weingartner, K.; Kohler, H. H.; Bittinger, A. Assessment of the vascularization in prostatic carcinoma: a morphometric investigation. *Hum. Pathol.* **1996**, *27* (12), 1306−10.

(31) Buckley, D. L.; Roberts, C.; Parker, G. J.; Logue, J. P.; Hutchinson, C. E. Prostate cancer: evaluation of vascular characteristics with dynamic contrast-enhanced T1-weighted MR imaging–initial experience. *Radiology* **2004**, *233* (3), 709−15.

(32) Pruijn, F. B.; Sturman, J. R.; Liyanage, H. D.; Hicks, K. O.; Hay, M. P.; Wilson, W. R. Extravascular transport of drugs in tumor tissue: effect of lipophilicity on diffusion of tirapazamine analogues in multicellular layer cultures. *J. Med. Chem.* **2005**, *48* (4), 1079−87.

(33) Virtual Computational Chemistry Laboratory. http://www.vcclab.org/lab/alogps/start.html (accessed April 2014).

(34) Sugano, K.; Kansy, M.; Artursson, P.; Avdeef, A.; Bendels, S.; Di, L.; Ecker, G. F.; Faller, B.; Fischer, H.; Gerebtzoff, G.; Lennernaes, H.; Senner, F. Coexistence of passive and carrier-mediated processes in drug transport. *Nat. Rev. Drug Discovery* **2010**, *9* (8), 597−614.

(35) Wajima, T.; Fukumura, K.; Yano, Y.; Oguma, T. Prediction of human pharmacokinetics from animal data and molecular structural parameters using multivariate regression analysis: volume of distribution at steady state. *J. Pharm. Pharmacol.* **2003**, *55* (7), 939−49.

(36) Cheng, L.; Jones, T. D.; Pan, C. X.; Barbarin, A.; Eble, J. N.; Koch, M. O. Anatomic distribution and pathologic characterization of small-volume prostate cancer (<0.5 mL) in whole-mount prostatectomy specimens. *Mod. Pathol.* **2005**, *18* (8), 1022−6.

(37) Radwanski, E.; Perentesis, G.; Symchowicz, S.; Zampaglione, N. Single and multiple dose pharmacokinetic evaluation of flutamide in normal geriatric volunteers. *J. Clin. Pharmacol.* **1989**, *29* (6), 554−8.

(38) Weinberg, B. D.; Patel, R. B.; Exner, A. A.; Saidel, G. M.; Gao, J. Modeling doxorubicin transport to improve intratumoral drug delivery to RF ablated tumors. *J. Controlled Release* **2007**, *124* (1−2), 11−9.

(39) Chowning, S. L.; Susil, R. C.; Krieger, A.; Fichtinger, G.; Whitcomb, L. L.; Atalar, E. A preliminary analysis and model of prostate injection distributions. *Prostate* **2006**, *66* (4), 344−57.

(40) Wientjes, M. G.; Zheng, J. H.; Hu, L.; Gan, Y.; Au, J. L. Intraprostatic chemotherapy: distribution and transport mechanisms. *Clin. Cancer. Res.* **2005**, *11* (11), 4204−11.